

## C<sub>60</sub> bonding and energy-level alignment on metal and semiconductor surfaces

T. R. Ohno, Y. Chen, S. E. Harvey, G. H. Kroll, and J. H. Weaver

*Department of Materials Science and Chemical Engineering, University of Minnesota, Minneapolis, Minnesota 55404*

R. E. Haufler and R. E. Smalley

*Rice Quantum Institute and Departments of Chemistry and Physics, Rice University, Houston, Texas 77251*

(Received 2 July 1991)

Electronic-structure studies of C<sub>60</sub> condensed on metal surfaces show that the energy levels derived from the fullerene align with the substrate Fermi level, not the vacuum level. For thick layers grown on metals at 300 K, the binding energy of the C 1s main line was 284.7 eV and the center of the band derived from the highest occupied molecular orbital was 2.25 eV below the Fermi level. For monolayer amounts of C<sub>60</sub> adsorbed on Au and Cr, however, the C 1s line was broadened asymmetrically and shifted to lower binding energy, the shakeup features were less distinct, and a band derived from the lowest unoccupied molecular orbital (LUMO) was shifted toward the Fermi level. These monolayer effects demonstrate partial occupancy of a LUMO-derived state, dipole formation, and changes in screening that are associated with LUMO occupancy. Results for C<sub>60</sub> monolayers on *n*-type GaAs(110) show transfer of  $\leq 0.02$  electron per fullerene, as gauged by substrate band bending. For C<sub>60</sub> on *p*-type GaAs, however, the bands remained flat because electron redistribution was not possible, and the C<sub>60</sub>-derived energy levels were aligned to the substrate vacuum level.

### INTRODUCTION

Several recent studies of solids derived from C<sub>60</sub> have focused on crystal structures<sup>1-3</sup> and electrical<sup>4,5</sup> and electronic<sup>6-8</sup> properties. The energy separation between the molecular highest occupied molecular orbital (HOMO) and lowest unoccupied molecular orbital (LUMO) levels<sup>9,10</sup> suggests that solid C<sub>60</sub> would behave like a semiconductor. For a van der Waals solid, such a small gap is remarkable.<sup>10</sup> Equally remarkable is the fact that solid C<sub>60</sub> is stable at much higher temperatures than other elemental van der Waals solids. Studies of the interaction of C<sub>60</sub> molecules with Au(111) have revealed close-packed structures derived from spherical objects separated by  $\sim 10$  Å.<sup>11</sup> In contrast, scanning tunneling microscopy (STM) studies of C<sub>60</sub> grown on GaAs(110) have shown distinct bonding sites.<sup>12</sup> Such studies raise questions as to the nature of the surface bond and the possibility that the molecules themselves could be altered by chemisorption processes.<sup>13</sup> Issues related to bonding and energy-level alignment are important in areas related to catalysis, oxidation, or electrochemistry with fullerenes.

This paper focuses on the interaction of C<sub>60</sub> with metal surfaces and with cleaved *n*- and *p*-type GaAs(110). Photoemission was used to measure the positions and line shapes of valence band and C 1s features; inverse photoemission was used to examine changes in the empty states associated with bonding. The metal substrates were chosen to provide a range of work functions and electronic character, namely the noble metals Ag and Au, the alkaline-earth metal Mg, the transition metal Cr, and the semimetal Bi. The results show that the energy levels of C<sub>60</sub> are aligned to the Fermi level for *all* of these metal surfaces, despite a work-function variation of  $\sim 1.5$  eV.

The C 1s line shapes for first-layer C<sub>60</sub> molecules reflect the extent of charge transfer and the character of surface bonds, in particular the mixing of the LUMO level with states of the metal substrate. Results for C<sub>60</sub> monolayers on *n*- and *p*-type GaAs(110) show no apparent surface chemistry but differences that were related to the position of the Fermi level in the gap. For these systems, charge transfer and substrate band bending was observed for *n*-type GaAs but not for *p*-type GaAs.

### EXPERIMENT

The x-ray-photoemission (XPS) measurements were carried out in an ultrahigh-vacuum system with monochromatized Al *K*α x rays focused to  $\sim 150$ -μm-diameter spots.<sup>14</sup> A hemispherical analyzer with a resistive anode was used to detect the emitted electrons. The instrumental broadening was 0.6 eV full width at half maximum (FWHM) when the pass energy was 25 eV, as determined from the Au 4*f*<sub>7/2</sub> emission. All core-level energies were referenced to the Fermi level of the grounded substrate. The synchrotron-radiation photoemission experiments were done at Aladdin using a spectrometer optimized for studies of overlayer growth in ultrahigh vacuum. Photoelectrons were collected with an angle-integrated double-pass cylindrical mirror analyzer. The overall instrumental resolution for the valence-band spectra was  $\sim 0.35$  eV. For the inverse-photoemission measurements,<sup>15</sup> a monoenergetic electron beam was incident on the sample and subsequent radiative transition from high-lying to lower-energy states produced photons with energies equal to the difference of the initial and final electronic states. Those photons were dispersed with a grating monochromator, and their energy distribution was measured in the

photon energy range 10–44 eV. The operating pressure was  $<4 \times 10^{-11}$  Torr during photoemission or inverse-photoemission data acquisition and  $<2 \times 10^{-10}$  Torr during  $C_{60}$  or metal deposition for all three systems.

Clean metal layers that could be used as substrates were grown by vapor condensation on cleaved GaAs(110) or on cleaved highly oriented pyrolytic graphite (HOPG). Mirrorlike GaAs(110) surfaces (*n*-type doped with Si at  $2 \times 10^{18} \text{ cm}^{-3}$  and *p*-type doped with Zn at  $2 \times 10^{18} \text{ cm}^{-3}$ ) were prepared by cleaving  $2 \times 4 \times 10 \text{ mm}^3$  posts. STM studies of the growth and properties of Bi, Mg, and Ag films on GaAs(110) have shown that these overlayers form by the coalescence of metal clusters.<sup>16–18</sup> Studies of Au and Cr overlayers on HOPG have also shown the merging of clusters into a layer that covers the surface.

The fullerenes were formed by the contact-arc method, with subsequent separation by solution with toluene.<sup>19</sup> Pure  $C_{60}$  was obtained by a liquid chromatography process on alumina diluted with mixture of hexanes. The resulting  $C_{60}$  was then rinsed in methanol, dried, and placed in Ta boats that were  $\sim 10$  cm from the substrate onto which the molecules were to be deposited. Degassing to  $\sim 475^\circ\text{C}$  desorbed residual solvents and condensates.  $C_{60}$  was sublimed at  $\sim 550^\circ\text{C}$ . The typical deposition rate of 0.5 Å per minute was measured with a quartz microbalance. We define one monolayer (ML) of  $C_{60}$  to be the equivalent of  $1.15 \times 10^{14}$  molecules/cm<sup>2</sup>. The thickness layer is 8 Å based on the bulk density of 1.65 g/cm<sup>3</sup> and the layer spacing for a close-packed solid.

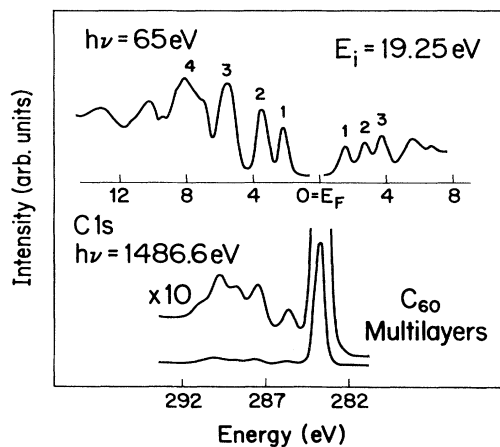


FIG. 1. The upper panel shows the distribution of occupied and empty electronic states for multilayer  $C_{60}$  measured with soft x-ray photoemission and inverse photoemission, respectively. The spectra were normalized so that the total intensity of the LUMO-derived peak was 60% of the HOMO-derived peak, reflecting the fivefold and threefold degeneracy of those levels. A quantitative correlation between the height of a given feature and the density of states should not be inferred (see Refs. 6 and 7). The HOMO-LUMO separation was 3.7 eV for the solid. The lower panel shows the C 1s main line and  $\pi$ - $\pi^*$  shakeup peaks.

## RESULTS AND DISCUSSION

### Electronic properties of $C_{60}$

Figure 1 shows the distribution of occupied and empty electronic states referenced to the Fermi level of the grounded spectrometers. The 50–100-Å-thick films grown on GaAs(110) at 300 K gave results that were representative of the bulk fullerite.<sup>6,7</sup> Scanning tunneling microscopy studies have revealed the surface morphology of such films.<sup>12</sup> Photoemission produced spectra that reflected the removal of an electron from the *N*-electron molecular system, while in inverse-photoemission results represented the addition of an electron. The valence-band results (upper panel) show well-defined features derived from the  $\pi_p$ ,  $\sigma_p$ , and  $\sigma_s$  levels. The leading occupied-state features, labeled 1 and 2, are  $\pi$  states that have radial charge densities characterized by a node in the “spherical” shell formed by the atomic nuclei.<sup>8</sup> These states form narrow bands in the small Brillouin zone of solid  $C_{60}$ . The deeper features have increasing  $\sigma_s$  and  $\sigma_p$  character and are more localized. The first two empty-state features are again  $\pi$  derived, with greater delocalization and more solid-state band character.

The lower panel of Fig. 1 shows the C 1s main line emission at 285.0 eV relative to  $E_F$  with  $\pi$ - $\pi^*$  shakeup features that extend to at least 7 eV higher energy. Broad plasmon loss structures associated with collective excitations of the charge of individual molecules can also be seen at  $\sim 18$  and 28 eV.<sup>6</sup> Analysis of the C 1s main line of Fig. 1 yields a Lorentzian of  $\sim 0.1$  eV. The width of the main line is then nearly instrument limited, and this provides evidence that all of the carbon sites are spectroscopically equivalent in the condensed fullerite. It is interesting to note that the shakeup features of Fig. 1 are analogous to those observed for aromatic compounds, but equivalent structures are not present in spectra for diamond or graphite.<sup>6</sup> They can be described as excited states of the molecule due to the change in the potential with the creation of a 1s core hole. The energies of these excited states of the  $N - 1$  electron system can be approximated by ground-state energies with valence electron promotion to an empty state. The shakeup feature at 1.9 eV corresponds to electron promotion from HOMO to LUMO.<sup>6</sup>

Figure 2(a) depicts the energy levels for isolated and solid  $C_{60}$ , the levels corresponding to the ionization potential (IP) and the electron affinity (EA) are 7.6 and 2.7 eV below the vacuum level  $E_{\text{vac}}$ .<sup>9</sup> For the solid, the removal or addition of an electron reveals the HOMO- and LUMO-derived bands with a difference in energy of 3.7 eV, as measured in Fig. 1 and depicted in Fig. 2(a). This is 1.2 eV less than the difference of IP and EA because of solid-state screening of the system established by electron removal or addition. For a van der Waals solid with no free carriers, this screening is due to charge polarization in the surrounding medium. For  $C_{60}$ , the wave function (charge distributions) describing the HOMO and LUMO levels are of comparable spatial extent so that the screening response should be nearly the same for electron removal or addition. The magnitude of the screening depicted

in Fig. 2(a) is consistent with solid C<sub>60</sub> having a static dielectric behavior close to that of graphite. To a first approximation, then, the hole (electron) is localized on a single molecule during the photoemission or inverse-photoemission process. If this were not the case and there were complete delocalization, the measured band gap would be very close to the "one-electron" or independent-particle HOMO-LUMO separation of  $\sim 1.6$  eV, free of many-body final-state effects. The ground state of the  $N$ -electron system depicted in Fig. 2 is consistent with calculations for the isolated molecule that predict rigid shifts of  $\sim 3$  eV for the energy levels of C<sub>60</sub><sup>+</sup> and C<sub>60</sub><sup>-</sup> relative to C<sub>60</sub>.<sup>20</sup>

Figure 2(a) gives plausible positions for the energy levels of C<sub>60</sub> in the ground state and in the measured final

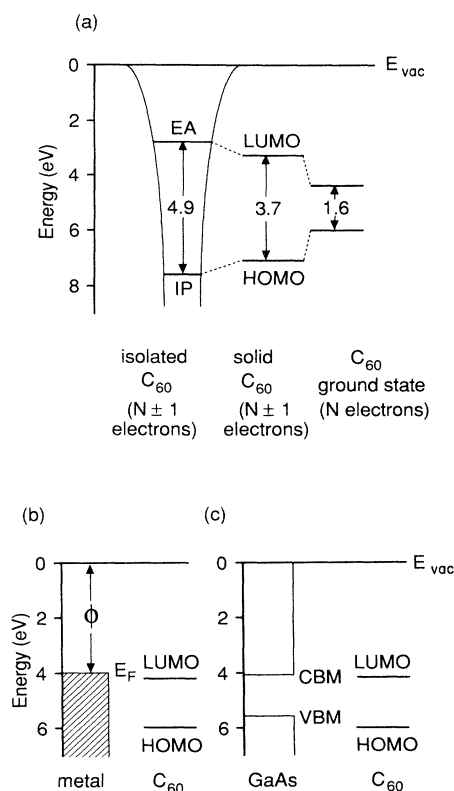


FIG. 2. (a) Energy-level diagram referenced to the vacuum level  $E_{vac}$  for isolated C<sub>60</sub> showing the ionization potential (IP) and the electron affinity (EA) levels and for the solid showing the LUMO- and HOMO-derived bands. The ground state of C<sub>60</sub> with  $N$  electrons is depicted at the right. Energy shifts for the solid and the molecule reflect the screening of the  $N+1$  (inverse photoemission) and  $N-1$  (photoemission) electron systems. We have assumed that the shifts are symmetric. (b) Energy-level diagram for C<sub>60</sub> condensed on a metal with a work function,  $\phi$  of 4 eV, assuming vacuum level alignment. In this case, the LUMO lies below  $E_F$ , suggesting charge mixing with the metal. (c) Energy-level diagram for C<sub>60</sub> condensed on GaAs(110) assuming vacuum level alignment. The proximity of the LUMO and the CBM suggests coupling with substrate electrons for  $n$ -type samples, as is shown to be the case.

states. The ground-state energies are needed to explain the trend in surface bonding and final-state screening on various substrates. Figure 2(b) again shows the ground-state energies for C<sub>60</sub> and depicts their alignment with a metal, assuming vacuum level alignment. For a metal with a work function of 4 eV, the ground-state energy of HOMO would then be  $\sim 1.9$  eV below  $E_F$  and LUMO would be near  $E_F$ . The relative energy positions of  $E_F$  and LUMO would suggest charge transfer to LUMO might be possible, depending on the work function. In a simple quantum-mechanical perturbation treatment of bond formation for adsorbates on metal substrates, mixing could occur between states with similar energies and would result in incremental charge transfer to LUMO.

Figure 2(c) reproduces the ground-state energies for C<sub>60</sub>, this time in contact with GaAs where the electron affinity is 4.1 eV and the energy gap is 1.4 eV. Vacuum level alignment would place HOMO below the valence-band maximum (VBM) and LUMO below the conduction-band minimum (CBM) in the semiconductor band gap. In this case, charge transfer to the adsorbed molecules would involve conduction-band electrons and would depend on whether the semiconductor is doped  $n$ -type or  $p$ -type. For  $n$ -type substrates, one might expect band-bending changes that would reflect such coupling. Such possibilities are explored in detail in the following.

#### Energy-level alignment on metal surfaces

The above discussion explicitly assumed that the metal work function  $\phi$  was 4 eV and that the common energy level was the vacuum level. Such an assumption of vacuum level alignment would be valid for large gap van der Waals solids, where the empty states are far above  $E_F$ . Indeed, photoemission from an adsorbed layer of Xe has been used to determine local work functions of various surfaces.<sup>21</sup> For C<sub>60</sub>, however, the LUMO is close to  $E_F$  and LUMO mixing can occur. To investigate the details of C<sub>60</sub> bonding, we undertook studies of monolayer and multilayer growth on metals with a range of work functions, namely Mg ( $\phi = 3.6$  eV), Bi ( $\phi = 4.2$  eV), Cr ( $\phi = 4.5$  eV), Ag ( $\phi = 4.3$  eV), and Au ( $\phi = 5.1$  eV).<sup>22</sup>

Figure 3 shows photoemission valence-band spectra for C<sub>60</sub> condensed on a 120-Å-thick Bi layer. The bottom energy distribution curve (EDC) shows Bi 6*p* emission within  $\sim 5$  eV of  $E_F$  and broad Bi 6*s* emission centered at  $\sim 11$  eV. The spectrum obtained after  $\sim 0.3$ -ML C<sub>60</sub> deposition reveals emission from molecular-orbital-derived features superimposed on attenuated emission from Bi. The C<sub>60</sub> features then grew in relative intensity but their energy positions remained unchanged. The center of the feature derived from HOMO was 2.3 eV below  $E_F$  for 2 ML.

The inset of Fig. 3 shows an EDC obtained after 2-ML C<sub>60</sub> deposition onto 30 Å Ag. Although the strong Ag *d*-band emission precluded quantitative examination of the C<sub>60</sub> monolayer features in the region 4–8 eV below  $E_F$ , the HOMO-derived band for  $\sim 2$  ML was clearly evident at 2.2 eV below  $E_F$ . (The spectra for C<sub>60</sub>/Ag were taken with  $h\nu = 110$  eV because the Cooper minimum in the 4*d* cross section suppressed substrate emission.)

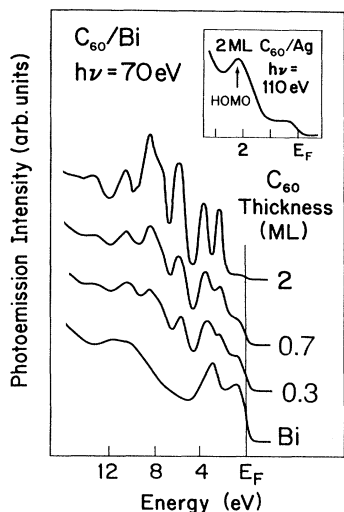


FIG. 3. Valence-band spectra for  $C_{60}$  condensed on Bi in the amounts given. The spectra are referenced to  $E_F$ , and they are plotted in arbitrary units. The inset shows the equivalent spectrum for 2-ML  $C_{60}$  condensed on Ag. For Ag and Bi, the HOMO-derived bands are centered 2.2–2.3 eV from  $E_F$ .

Figure 4 shows EDC's for  $C_{60}$  condensed on a 300-Å-thick Mg film. The Fermi-level cutoff was clearly seen in the Mg spectrum and the broad structure beneath the Mg  $sp$  band was due to Auger  $LVV$  emission ( $h\nu = 70$  eV, Mg  $2p$  binding energy  $\sim 50$  eV). As with Bi, all of the molecular features are visible for 0.7-ML deposition. The

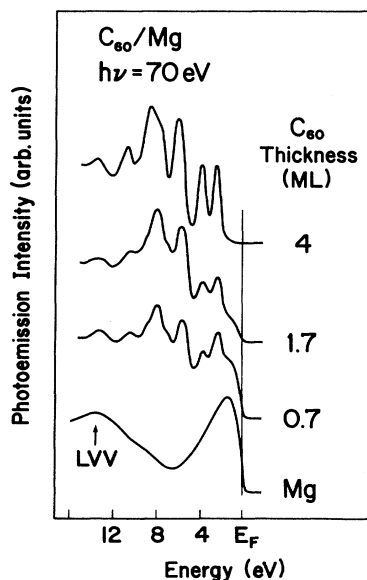


FIG. 4. Valence-band spectra for  $C_{60}$  condensed on Mg showing the growth of the  $C_{60}$  features with the HOMO 2.2 eV below  $E_F$ .

$C_{60}$  molecular features then grew relative to the weak Mg emission and, again, the HOMO was 2.2 eV below  $E_F$ . The deposition of 4 ML at 300 K produced valence-band features that were identical to those of bulk  $C_{60}$ .

Figure 5 shows the C 1s emission as a function of  $C_{60}$  deposition on Au. The C 1s main line for 0.5 ML showed a broadening by 0.25 eV relative to that for a thick layer (Fig. 1), a line-shape asymmetry to higher binding energy, and an 0.4-eV shift to 284.6 eV. The  $\pi-\pi^*$  satellite features were also broader, and the HOMO-LUMO satellite at 1.9 eV was obscured by the main line. Increasing the coverage to 1 ML resulted in a sharpening of the main line, a shift to higher energy, and more distinct shakeup features. STM investigations of the surface morphology for  $\sim 1$ -ML  $C_{60}$  on Au show a first  $C_{60}$  layer but also second layers and open patches.<sup>11,12</sup> Photoemission line-shape analysis in terms of contributions from the first layer (dashed line) and subsequent layers suggests that  $\sim 35\%$  of the surface had single-layer coverage, while an equal amount was at least two molecules thick for growth at 300 K.

Figure 6 shows the C 1s emission for growth on Cr. Analysis again reveals asymmetric line shapes for fullerenes in contact with the metal. Significantly, the main line appeared at 284.2 eV, well shifted relative to growth on Au and the shakeup features were nearly undifferentiated. The main line could be decomposed into emission from the first layer (dashed line) and the second layer, as shown. By  $\sim 2$  ML, the shakeup peaks were clearly visible, with the 1.9-eV feature well resolved from the now-sharper main line. Multilayer emission was

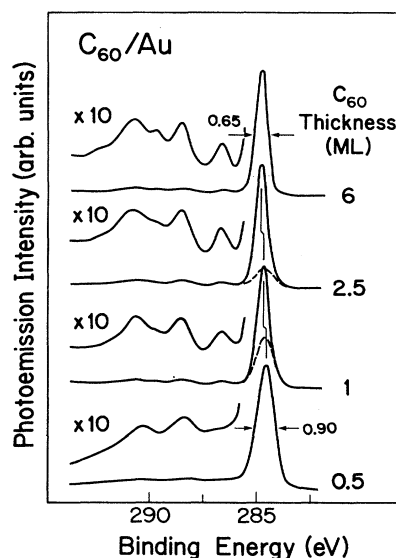


FIG. 5. C 1s spectra for  $C_{60}$  condensed on Au showing main line sharpening and satellite development for multilayers compared to the first layer. Analysis indicates that second-layer islands start to form by  $\sim 1$ -ML deposition and the C 1s energy position for molecules in second and subsequent layers differ from those in the first layer (dashed line).

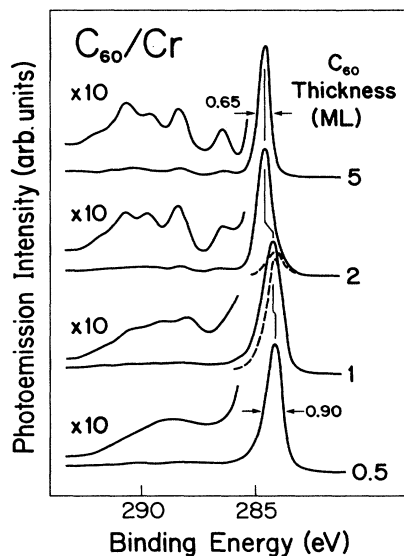


FIG. 6. C 1s spectra for C<sub>60</sub> deposition on Cr, as in Fig. 5.

indistinguishable from that of bulk C<sub>60</sub>, although the main line appeared at  $284.6 \pm 0.1$  eV for growth on Cr and  $284.8 \pm 0.1$  eV for growth on Au.

The results of Figs. 3–6 demonstrate that the peak in the HOMO-derived band is 2.2–2.3 eV below  $E_F$  and the C 1s main line is at 284.6–284.8 eV for C<sub>60</sub> multilayers, despite the  $\sim 1.5$ -eV variation in the metal work functions. Hence, the energy levels of thick fullerene layers align with the Fermi level of the substrate, not the vacuum level. This energy reference is established by a redistribution of charge and the formation of an interface dipole. We estimate that the first-layer fullerenes have 0.1–0.5 additional electronic charge per molecule to compensate for the metal work functions, based on a model that assumes charged planes separated by 5 Å, the fullerene radius. As discussed below, analogous effects are observed for CO adsorption on metal surfaces where a broad  $2\pi$ -derived resonance appeared near  $E_F$ .<sup>23–25</sup>

#### Energy-level alignment on GaAs(110)

C<sub>60</sub> adsorption on GaAs(110) gives quite different results from those for metals because the bulk semiconductor Fermi level lies near the CBM or VBM, depending on dopant type. As shown in Fig. 7 for 0.5- and 6-ML films on GaAs(110), the C 1s core-level results were essentially identical, in contrast to results for metallic surfaces. Adsorption on *n*-type GaAs gave a C 1s main line binding energy of 285.0 eV and the HOMO was located  $2.4 \pm 0.1$  eV below  $E_F$ , both  $\sim 0.2$  eV deeper than for thick layers on metals. The shakeup features were clearly visible for 0.5 ML on GaAs, although they were distorted by overlap with As LMM Auger emission. Analysis of the sub-

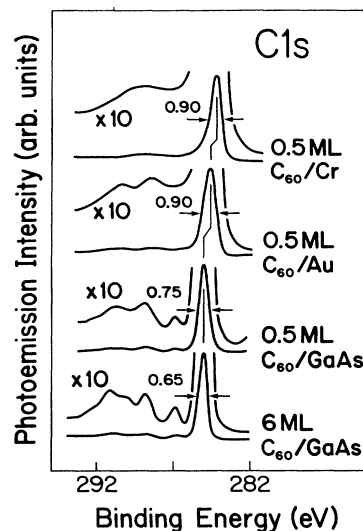


FIG. 7. Comparison of C 1s spectra for first-layer C<sub>60</sub> on Cr, Au, and GaAs showing differences in energy and width for the main line and differences in appearance for the satellite structures. The results for 6 ML on GaAs are representative of thick films.

strate core-level features showed an adsorbate-induced band bending of 0.3 eV for *n*-type GaAs(110). Analysis also showed that there were no changes in surface relaxation and no new bonding configurations were formed at the interface. The 0.3-eV band bending for GaAs doped at  $2 \times 10^{18}$  cm<sup>-3</sup> required the formation of an interface dipole and a depletion region  $\sim 150$  Å thick. A dipole with charge transfer from the semiconductor implies that the LUMO falls below the GaAs CBM. In turn, the 0.3-eV shift implies charge transfer of only  $\sim 3 \times 10^{12}$  electrons/cm<sup>2</sup>, or  $\sim 0.02$  electron per first layer fullerene, as weak mixing of the conduction band and the LUMO level occurs. These changes are depicted in Fig. 8, where the dashed lines denote the ground-state energies of the LUMO and the HOMO and the solid lines represent observed values, shifted because an electron was added or removed. Also shown is the depletion region and the 0.3-eV surface barrier.

The lower portion of Fig. 8 shows the results for C<sub>60</sub> adsorption onto *p*-type GaAs(110). In this case, there was no measurable change in band bending. The HOMO and the C 1s main line appeared at 1.6 and 284.3 eV, shifted  $\sim 0.8$  eV relative to *n*-type GaAs(110) with no changes in line shape. The absence of adsorbate-induced band bending or charge transfer shows that the C<sub>60</sub> energies were strictly vacuum referenced. Thus, the LUMO is well above the surface Fermi level and the HOMO falls in the GaAs valence band (Fig. 8). Since C<sub>60</sub> and GaAs(110) are vacuum referenced, the ionization potential of solid C<sub>60</sub> is 7.1 eV, as shown in Fig. 8. This agrees well with values estimated above, where we assumed symmetric screening in the ( $N-1$ ) and ( $N+1$ ) systems of Fig. 2(a).

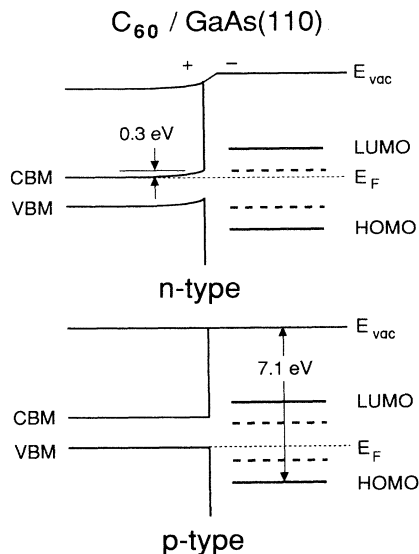


FIG. 8. Energy-level diagram for  $C_{60}$  on *n*- and *p*-type GaAs. Dashed lines represent ground-state energies and solid lines denote the measured energies. Deposition on *n*-type GaAs(110) produced a 0.3-eV Fermi-level shift from the CBM, indicating net charge transfer from the semiconductor to the resonance state derived from the LUMO. The HOMO was 2.4 eV below  $E_F$  and the C 1s main line appeared at 285.0 eV. Deposition on *p*-type caused no band bending, the HOMO was 1.6 eV below  $E_F$ , and the C 1s main line appeared at 284.3 eV. The differences reflect the inability of carriers to couple to  $C_{60}$  for *p*-type GaAs and vacuum level referencing.

#### $C_{60}$ substrate bonding

Figure 7 shows the C 1s emission obtained after deposition of  $\sim 0.5$ -ML  $C_{60}$  on Cr, Au, and *n*-type GaAs(110), as well as for a 6-ML film on GaAs. The thickness-dependent results for GaAs(110) reveal broadening by 0.1 eV of the C 1s main line for 0.5 ML. Again, these results indicate that there was little modification of the  $C_{60}$  layer in contact with the semiconductor and that bonding was dominated by van der Waals interactions. In contrast, the submonolayer results of Fig. 7 for Au were characterized by a C 1s main line shifted by  $\sim 0.2$  eV from the peak for thick layers on metals, a broadening by 0.25 eV, and an asymmetry to higher binding energy (asymmetry parameter  $\alpha=0.09$ ). Although the shakeup features were evident, they too were broadened and the background was substantially higher than for multilayer films. The 1.9-eV  $\pi$ - $\pi^*$  feature could not be detected. For  $\sim 0.5$  ML of  $C_{60}$  on Cr, the C 1s main line was shifted 0.4 eV relative to that for thick layers on Cr, the main line was broadened and even more asymmetric ( $\alpha=0.12$ ), and the shakeup features were replaced by a broad feature. These results for adsorption on metal surfaces demonstrate that bonding is not simply van der Waals.

Additional insight into surface bonding can be gained from the inverse-photoemission results shown in Fig. 9 for low coverages of  $C_{60}$  on Au. The peaks superimposed

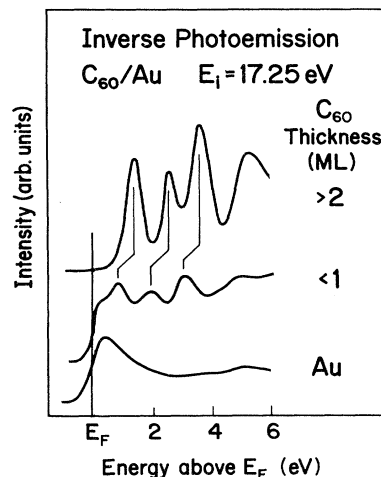


FIG. 9. Empty state spectra obtained with inverse photoemission for  $C_{60}$  on Au showing a shift in energy for the monolayer results relative to those for thicker layers because of first-layer mixing of LUMO with Au substrate levels.

on the Au conduction-band emission are analogous to those of Fig. 1 but the submonolayer features were shifted  $\sim 0.5$  eV toward  $E_F$ . Since photoemission results showed that the HOMO-derived band did not move, this implies that the HOMO-LUMO separation was reduced from 3.7 to 3.2 eV, an effect related to hybridization between the LUMO and the metal states (discussed below).

The results for  $C_{60}$  adsorption on metals can be examined from the perspective of chemisorption literature, particularly that related to CO adsorption on metals.<sup>23–25</sup> For nondissociative CO bonding to a metal surface (with the C atom down), theoretical discussions have focused on perturbative treatments of the molecular orbitals. CO hybridization with small metal clusters to form bonding and antibonding levels has been considered, as has hybridization with a band of metal states to form a broad resonance.<sup>23–25</sup> In the latter, the resonance derived from empty  $2\pi$  orbitals and the metal band was centered above  $E_F$  but its tail extended below  $E_F$ . The result was a small increase in charge density near the CO molecule due to partial occupancy of the  $2\pi$  orbitals without substantial modification.<sup>23–25</sup> Analysis showed that the  $2\pi$  charge density was beyond the metal dipole layer and that the next empty levels were sufficiently high in energy that they could not mix.

The experimental result for  $C_{60}$  adsorbed on metal surfaces indicates that the amount of charge transfer is small, but not negligible, compared to the number of valence electrons per molecule, and that the reduced molecular symmetry associated with condensation did not significantly change the distribution of occupied electronic states. Hence, a perturbation treatment is reasonable. We propose, therefore, that mixing between the LUMO and filled metal states produces a resonance that is centered above  $E_F$  but has a tail that accommodates sufficient charge to produce Fermi-level alignment. This charge would reside in a state that looks very much like

the LUMO. Polarization of charge on the molecule and deviation from spherical character should be small.

Figure 10 shows the proposed energy-level diagram for C<sub>60</sub> monolayers and multilayers adsorbed on a metal. Measured LUMO- and HOMO-derived peak positions are represented by broad solid lines. They are shifted from the ground-state positions (indicated by dashed lines) by final-state effects related to the addition or removal of an electron. For a monolayer of C<sub>60</sub>, the ground-state LUMO-derived level is "pinned" nearer the Fermi level than the LUMO for thicker layers, since it is partially occupied. This shift toward  $E_F$  is enhanced by screening of the photohole by image charges and polarization screening by adjacent fullerenes. In the ground state the HOMO will follow the LUMO, since C<sub>60</sub> molecular levels are not changed substantially by bonding with the substrate. Thus, the ground state will shift for the first monolayer, as depicted in Fig. 10. In contrast, screening of the HOMO in the photoemission final state caused by the substrate image charge will tend to shift the observed position toward  $E_F$ . For the HOMO, these two effects are largely offsetting and there is no significant change in the measured HOMO position for growing films.

For fullerenes in thick molecular layers, alignment of their ground-state energies is determined by the interface dipole, i.e., bond formation in the first layer, which assured alignment to the substrate  $E_F$ . Screening of the  $N-1$  and  $N+1$  final states of photoemission and inverse photoemission is only by polarization of the molecular environment, and this is independent of the metal substrate. Interactions between first layers and subsequent layers are mostly van der Waals, since the first layer is

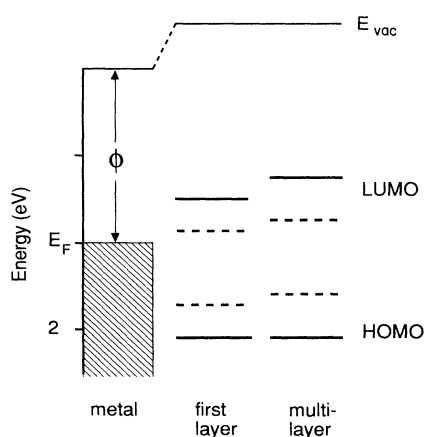


FIG. 10. Energy-band picture for first layer and multilayer C<sub>60</sub> on a metal with work function  $\phi$ . Dashed lines represent ground-state energies. The solid lines depict measured energies for photoemission ( $N-1$  system) and inverse photoemission ( $N+1$  system). The ground-state mixing of the LUMO with metal levels produces a dipole that aligns the Fermi level. That mixing shifts the ground-state LUMO level toward  $E_F$ . The apparent reduction in the HOMO-LUMO gap reflects final-state screening of the hole or added electron.

not modified much by substrate bonding. Therefore, the observed energy positions for valence and core-level features will be the same for C<sub>60</sub> multilayers on all metals, and they will be aligned to the substrate  $E_F$ , as observed.

It is interesting to note that the C 1s-HOMO separation decreases by 0.2–0.4 eV for a C<sub>60</sub> monolayer relative to a multilayer. For any adsorbed molecule, the creation of a C 1s core hole causes all levels to shift to higher binding energy as each level is more tightly bound by a nucleus that is no longer screened by a filled 1s shell. The removal of an electron from a valence state has a small effect because of its much larger spatial extent. For a molecule in contact with the metal surface, the creation of the core hole pulls the LUMO-metal resonance toward  $E_F$  and charge transfer from the substrate to LUMO-derived states contributes additional screening for the C 1s hole. The magnitude of the shift due to charge-transfer screening for first layer and multilayers is approximately the C 1s binding-energy difference for thick and thin films, namely 0.2 eV for Au and 0.4 for Cr. The larger shift for C<sub>60</sub> on Cr reflects stronger LUMO-metal interaction in the ground state and hence larger charge-transfer screening in the final state. We note that analogous screening has been observed for CO and benzene on transition metals, where the shift has been shown to vary with substrate bonding strength.<sup>24,26</sup>

The observed changes in the width of the C 1s main line for monolayers and multilayers can again be understood by analogy with adsorbed molecules, where the response to the core hole reflects the ground-state hybrids between metal states and the LUMO.<sup>24,27,28</sup> In this case, the C 1s linewidth is related to the increased width of the LUMO-derived resonance (the greater the mixing, the shorter the lifetime). Effects related to image charge screening in the final state appear to play a minor role in determining the line shape because they should be observed for GaAs as well as metals, but they were not. The suggestion that core holes created in carbon atoms nearer the substrate would be screened more effectively than those on the outer edge can be discarded, since this would introduce an asymmetry to lower binding energy. Indeed, we can assume that all C 1s core holes are equivalent for screening by charge transfer from the substrate because the LUMO level has the symmetry of the molecule. Finally, the pronounced asymmetry of the C 1s main line is a result of low-energy losses for the photoemitted electron<sup>24</sup> and it reflects the density of the LUMO-metal hybrids at  $E_F$ . Such lifetime broadening and asymmetries have been observed for CO and benzene chemisorbed on transition metals.<sup>24,28</sup>

Differences in the shakeup structures for first-layer C<sub>60</sub> molecules also indicate LUMO mixing with Cr and Au. Umbach<sup>29</sup> has shown that physisorbed molecules retain the shakeup structures observed in the gas phase because the final states involve only molecular orbitals with broadening due to the substrate screening response. For strongly chemisorbed molecules, the sharp molecular features are replaced by structureless satellites because of mixing of molecular and substrate levels in the initial and final states.<sup>30</sup> The results of Fig. 7 show a broad main line and a satellite at  $\sim 6$ -eV higher binding energy for

C<sub>60</sub> adsorbed on Cr, consistent with relatively strong interaction. In contrast, those for C<sub>60</sub> adsorbed on Au show more distinct satellites, and those for GaAs exhibit essentially unchanged molecular final states.

### SUMMARY

The spectral results described here for C<sub>60</sub> multilayers can be understood in terms of localization of the photohole or added electron on a molecule in a dielectric medium with shifts from the ground-state energies due to polarization of the van der Waals solid. Adsorption of C<sub>60</sub> monolayers on metals results in charge transfer and LUMO-metal state mixing that assures Fermi-level alignment and accounts for additional bonding beyond van der Waals bonding. For these monolayers, we observe changes in the C 1s energy and line shape that reflect the LUMO-metal hybrid states, since they are involved in the many-body relaxation and decay of the core hole.<sup>31</sup> For C<sub>60</sub> adsorbed on GaAs, the energy-level alignment de-

pends on the dopant type because the LUMO lies near the CBM, and coupling with the LUMO requires electrons in the conduction band. Only when mixing of states of the substrate with LUMO is not possible are the vacuum levels aligned, as is the case for larger gap van der Waals solids. Such is the case for C<sub>60</sub> on *p*-type GaAs(110).

### ACKNOWLEDGMENTS

This work was supported by the Office of Naval Research, the National Science Foundation, and the Robert A. Welch Foundation. The inverse-photoemission results were generously provided by M. B. Jost and D. M. Poirier. Discussions with J. L. Martins, N. Troullier, G. D. Waddill, and Y. Z. Li are gratefully acknowledged. Some of the photoemission studies were performed at the Wisconsin Synchrotron Radiation Center, a user facility operated by the University of Wisconsin for the National Science Foundation.

- <sup>1</sup>R. Fleming *et al.*, in *Clusters and Cluster Assembled Materials*, edited by R. S. Averback, J. Bernhole, and D. L. Nelson, MRS Symposia Proceedings No. 206 (Materials Research Society, Pittsburgh, 1991), p. 691.
- <sup>2</sup>P. A. Heiney, J. E. Fischer, A. R. McGhie, W. J. Romanow, A. M. Denenstein, J. P. McCauley, Jr., A. B. Smith III, and D. E. Cox, *Phys. Rev. Lett.* **66**, 2911 (1991); O. Zhou *et al.*, *Nature* **351**, 462 (1991); P. W. Stephens, L. Mihaly, P. L. Lee, R. L. Whetten, S.-M. Huang, R. Kaner, F. Diederich, and K. Holczer, *ibid.* **351**, 632 (1991).
- <sup>3</sup>J. M. Hawkins, A. Meyer, T. A. Lewis, S. Loren, and F. J. Holczer, *Science* **252**, 312 (1991).
- <sup>4</sup>R. C. Haddon *et al.*, *Nature* **350**, 320 (1991).
- <sup>5</sup>A. F. Hebard, M. J. Rosseinsky, R. C. Haddon, D. W. Murphy, S. H. Glarum, T. T. M. Palstra, A. P. Ramirez, and A. R. Kortan, *Nature* **350**, 600 (1991); M. J. Rosseinsky *et al.*, *Phys. Rev. Lett.* **66**, 2830 (1991); K. Holczer, O. Klein, S.-M. Huang, R. B. Kaner, K.-J. Fu, R. L. Whetten, and F. Diederich, *Science* **252**, 1154 (1991); P. J. Benning, J. L. Martins, J. H. Weaver, L. P. F. Chibante, and R. E. Smalley, *ibid.* **252**, 1417 (1991).
- <sup>6</sup>J. H. Weaver, J. L. Martins, T. Komeda, Y. Chen, T. R. Ohno, G. H. Kroll, N. Troullier, R. E. Haufler, and R. E. Smalley, *Phys. Rev. Lett.* **66**, 1741 (1991). See also D. L. Lichtenberger, M. E. Jatcko, K. W. Nebesny, C. D. Ray, D. R. Huffman, and L. D. Lamb, *Chem. Phys. Lett.* **176**, 203 (1991); P. J. Benning, D. M. Poirier, N. Troullier, J. L. Martins, J. H. Weaver, R. E. Haufler, L. P. F. Chibante, and R. E. Smalley, *Phys. Rev. B* **44**, 1962 (1991).
- <sup>7</sup>M. B. Jost, N. Troullier, D. M. Poirier, J. L. Martins, J. H. Weaver, L. P. F. Chibante, and R. E. Smalley, *Phys. Rev. B* **44**, 1966 (1991).
- <sup>8</sup>Q. Zhang, J.-Y. Yi, and J. Bernholc, *Phys. Rev. Lett.* **66**, 2633 (1991); S. Saito and A. Oshiyama, *ibid.* **66**, 2637 (1991); J. L. Martins, N. Troullier, and J. H. Weaver, *Chem. Phys. Lett.* **180**, 457 (1991); J. W. Mintmire, B. I. Dunlap, D. W. Brenner, R. C. Mowrey, and C. T. White, *Phys. Rev. B* **43**, 14281 (1991).
- <sup>9</sup>S. H. Yang, C. L. Pettiette, J. Conceicao, O. Cheshnovsky, and R. E. Smalley, *Chem. Phys. Lett.* **139**, 233 (1987).
- <sup>10</sup>H. Ajie *et al.*, *J. Phys. Chem.* **94**, 8630 (1990).
- <sup>11</sup>R. J. Wilson, G. Meijer, D. S. Bethune, R. D. Johnson, D. D. Chambliss, M. S. deVries, H. E. Hunziker, and H. R. Wendt, *Nature* **348**, 621 (1990); J. L. Wragg, J. E. Chamberlain, H. W. White, W. Krätschmer, and D. R. Huffman, *ibid.* **348**, 623 (1990).
- <sup>12</sup>Y. Z. Li, J. C. Patrin, M. Chander, J. H. Weaver, L. P. F. Chibante, and R. E. Smalley, *Science* **252**, 547 (1991); Y. Z. Li, M. Chander, J. C. Patrin, J. H. Weaver, L. P. F. Chibante, and R. E. Smalley, *ibid.* **253**, 429 (1991).
- <sup>13</sup>T. Chen, S. Howells, M. Gallagher, L. Yi, D. Sarid, D. L. Lichtenberger, K. W. Nebesny, and C. D. Ray (unpublished).
- <sup>14</sup>S. A. Chambers, D. M. Hill, F. Xu, and J. H. Weaver, *Phys. Rev. B* **35**, 634 (1987).
- <sup>15</sup>Y. Gao, M. Gironi, B. Smandek, J. H. Weaver, and T. Tyrie, *J. Phys. E* **21**, 489 (1988).
- <sup>16</sup>See, for example, R. Ludeke, A. Taleb-Ibrahimi, R. M. Feenstra, and A. B. McLean, *J. Vac. Sci. Technol. B* **7**, 936 (1989).
- <sup>17</sup>Y. Z. Li, J. C. Patrin, Y. Chen, and J. H. Weaver, *Phys. Rev. B* **44**, 8843 (1991).
- <sup>18</sup>B. Trafas, Y.-N. Yang, R. L. Siefert, and J. H. Weaver, *Phys. Rev. B* **43**, 14107 (1991), and references cited therein.
- <sup>19</sup>R. E. Haufler *et al.*, *J. Phys. Chem.* **94**, 8634 (1990); R. E. Haufler, Y. Chai, L. P. F. Chibante, J. Conceicao, C. Jin, L.-S. Wang, S. Maruyama, and R. E. Smalley, in *Clusters and Cluster Assembled Materials* (Ref. 1), p. 627.
- <sup>20</sup>A. Rosen and B. Wästberg, *J. Chem. Phys.* **90**, 2525 (1989); S. Saito, in *Clusters and Cluster Assembled Materials* (Ref. 1), p. 115.
- <sup>21</sup>K. Wandelt, *J. Vac. Sci. Technol. A* **2**, 802 (1984); T.-C. Chiang, G. Kaindl, and T. Mandel, *Phys. Rev. B* **33**, 695 (1986).
- <sup>22</sup>*CRC Handbook of Chemistry and Physics*, 69th ed., edited by R. C. Weast (CRC, Boca Raton, 1988), E91-92.
- <sup>23</sup>Ph. Avouris, P. S. Bagus, and C. J. Nelin, *J. Electron Spectrosc. Relat. Phenom.* **38**, 269 (1986).
- <sup>24</sup>B. Gumhalter, K. Wandelt, and Ph. Avouris, *Phys. Rev. B* **37**, 8048 (1988); B. Gumhalter, *ibid.* **33**, 5245 (1986).
- <sup>25</sup>P. S. Bagus, C. J. Nelin, and C. W. Bauschlicher, *J. Vac. Sci.*

- Technol. A **2**, 905 (1984).
- <sup>26</sup>A. C. Liu and C. M. Friend, *J. Chem. Phys.* **89**, 4396 (1988); K. Kishi, F. Kikui, and S. Ikeda, *Surf. Sci.* **99**, 405 (1980); H. Hoffman, F. Zaera, R. M. Ormerod, R. M. Lambert, L.-P. Wang, and W. T. Tysoe, *ibid.* **232**, 259 (1990).
- <sup>27</sup>J. C. Fuggle, E. Umbach, D. Menzel, K. Wandelt, and C. R. Brundle, *Solid State Commun.* **27**, 65 (1978), and references cited therein.
- <sup>28</sup>E. W. Plummer, W. R. Salaneck, and J. S. Miller, *Phys. Rev. B* **18**, 1673 (1978).
- <sup>29</sup>E. Umbach, *Surf. Sci.* **117**, 482 (1982).
- <sup>30</sup>For CO chemisorbed on metals, the most intense shakeup feature is attributed to a final state arising from charge transfer from the metal and a broad satellite is due to an un-screened final state, as discussed in Ref. 28.
- <sup>31</sup>K. Schönhammer and O. Gunnarsson, *Solid State Commun.* **23**, 691 (1977).